Self-sustaining Positive Feedback Loops in Discrete and Continuous Systems

Jordan C. Rozum, Réka Albert

PII: S0022-5193(18)30453-3
DOI: https://doi.org/10.1016/j.jtbi.2018.09.017
Reference: YJTBI 9626

To appear in: *Journal of Theoretical Biology*

Received date: 5 May 2018
Revised date: 19 August 2018
Accepted date: 17 September 2018

Please cite this article as: Jordan C. Rozum, Réka Albert, Self-sustaining Positive Feedback Loops in Discrete and Continuous Systems, *Journal of Theoretical Biology* (2018), doi: https://doi.org/10.1016/j.jtbi.2018.09.017

Highlights

- Positive feedback in regulatory circuits can trap system in control-robust behavior
- Analysis of ODE models is informed by analogies with Boolean systems
- Subsystem behavior can place bounds on the effectiveness of system interventions

Self-sustaining Positive Feedback Loops in Discrete and Continuous Systems

Jordan C. Rozum*

Department of Physics, The Pennsylvania State University, University Park, PA, USA

Réka Albert

Department of Physics, The Pennsylvania State University, University Park, PA, USA

Department of Biology, The Pennsylvania State University, University Park, PA, USA

Abstract

We consider a dynamic framework frequently used to model gene regulatory and signal transduction networks: monotonic ODEs that are composed of Hill functions. We derive conditions under which activity or inactivity in one system variable induces and sustains activity or inactivity in another. Cycles of such influences correspond to positive feedback loops that are self-sustaining and control-robust, in the sense that these feedback loops "trap" the system in a region of state space from which it cannot exit, even if the other system variables are externally controlled. To demonstrate the utility of this result, we consider prototypical examples of bistability and hysteresis in gene regulatory networks, and analyze a T-cell signal transduction ODE model from the literature.

Keywords: biomolecular networks, network control, feedback, Boolean models, ODEs

1. Introduction

Feedback loops determine the dynamics of many biological systems (Albert and Othmer, 2003; Angeli et al., 2004; van Dassow, G. et al., 2000; Wittmann et al., 2009; Yao et al., 2014). The pioneering work of René Thomas and colleagues (Glass and Kauffman, 1973; Snoussi and Thomas, 1993; Thomas and Kaufman, 2001a,b) showed that certain qualitative features of a system's attractor repertoire are closely linked to the presence of positive or negative feedback loops. By considering the logical relationships between variables, as determined by the sign of entries in the Jacobian, René Thomas demonstrated that positive feedback loops are necessary for multistability. The question of whether multistability is realized in a system is reduced to the question of whether its positive feedback loops are "functional" (Snoussi and Thomas, 1993). René Thomas introduced the paradigm in which feedback loops, rather than individual elements, constitute the fundamental components of a system.

More recent work on the role of feedback loops in dynamical systems includes the method of feedback

*Corresponding Author
Email addresses: jcr52@psu.edu (Jordan C. Rozum), rza1@psu.edu (Réka Albert)

vertex set (FVS) control (Fiedler et al., 2013; Mochizuki et al., 2013). The key result of FVS control highlights the importance of feedback as a determinant of system fate: control of at least one variable in each feedback loop is sufficient to drive a continuous and bounded system into any of its attractors. Chemical reaction networks have also been analyzed in the context of feedback loops, and conditions for feedback loop functionality are known (Craciun and Feinberg, 2006; Shinar and Feinberg, 2010). The dynamical flexibility imparted by feedback loops has inspired a large body of research (e.g., Alves et al., 2014; Azpeitia et al., 2017; Bhalla and Iyengar, 1999; Pfeuty and Kaneko, 2009; Tian et al., 2013; Yeger-Lotem et al., 2004).

Such results are especially useful in modeling biological systems because these are often high-dimensional and subject to large uncertainties in parameter and variable values. Fortunately, there is increasing evidence that the connectivity of the system components and the sign of the influence among these components plays an important role, or even determines, the system's long-term dynamics. This insight, enabled in part by Thomas and Kaufman (2001a,b), encourages the implementation of simplified models, such as discrete models, that can draw broad, qualitative conclusions without involving many parameters. Discrete dynamical models have successfully modeled many biological systems, such as phenotypic changes in cells, metabolism, and population dynamics (Albert and Othmer, 2003; Collombet et al., 2017; Robeva and Murrugarra, 2016; Steinway et al., 2014; Veliz-Cuba and Stigler, 2011).

In Boolean models, certain positive feedback loops correspond to control-robust subsystems that maintain a steady state independent of the rest of the system (Zañudo and Albert, 2013, 2015). For the purposes of system control, these subsystems are viewed as fundamental units, in the spirit of Thomas' pioneering work on feedback (Thomas and Kaufman, 2001a,b). These results have been generalized to multi-level discrete systems (Gan and Albert, 2018), and we have recently generalized these Boolean results to continuous-valued systems (Rozum and Albert, 2018). Here, we apply this subsystem methodology to feedback loops in ordinary differential equations (ODEs) composed of Hill function regulation, with the aim of elucidating the shared role of positive feedback loops in Boolean and ODE systems.

We focus our attention on Hill function ODEs in particular for several reasons. First, they have well-established parallels with Boolean discrete-time systems (Krumsiek et al., 2010; Wittmann et al., 2009), which makes adaptation of Boolean results more straightforward. More generally, Hill functions have desirable analytical properties: they are continuous, bounded, and strictly monotonic. Furthermore, these ODEs have clear biomolecular motivations in gene regulatory networks (see e.g., Karlebach and Shamir, 2008; Mackey et al., 2016). Even when Hill functions are not directly motivated from a biological perspective, they may still be a reasonable choice for generic sigmoidal responses. Indeed, Hill function ODEs are frequently chosen as a first approximation for biomolecular systems when detailed dynamics are not known (e.g., Laslo et al., 2006; Wittmann et al., 2009).

We consider relationships between statements about the values of variables relative to certain thresholds. When these relationships form a cycle of compatible statements, the cycle describes a cyclic stable motif. A

cyclic stable motif is a subsystem that self-sustain its variables above or below their thresholds, independent from the rest of the system. We will show that cyclic stable motifs are always associated to positive feedback loops and describe state-space "trap" regions, that is, regions of state space that once entered, cannot be exited. Because cyclic stable motifs are self-sustaining, they must be directly controlled in order to drive the system into a desired state. Practically, this means that effective therapeutic interventions in biomolecular networks must target at least one member of every cyclic stable motif.

We will show, using toy examples, how cyclic stable motifs can be used to study multistability, hysteresis, and signal cross-talk in the context of system control and drug intervention in biomolecular networks. We will also demonstrate the identification of a cyclic stable motif in a T-cell signal transduction model from the literature (Wittmann et al., 2009).

2. Sufficient Positive Feedback in Boolean Models

Many systems are effectively modeled as Boolean networks, in which each system variable can take one of two values (1 for "on" or "active" and 0 for "off" or "inactive") at any given time. At each time step, a set of variables is selected for update according to a specified update schedule. Each variable, X_i, in the update set attains a new value X_i^* given by its regulatory function $f_i = f_i\left(X_1, X_2, ..., X_N\right)$.

An exhaustive search of the state space in these Boolean models is often impractical, as the number of states that must be considered scales exponentially with the number of variables. Several techniques have been proposed to identify important dynamical properties of Boolean systems without the need for a comprehensive search of the state space (Wang et al., 2012). We will focus on a special case of the methods presented by Zañudo and Albert (2013) and expanded upon by Gan and Albert (2018), which we will show generalizes to provide insights about positive feedback in continuous-valued systems.

Following Zañudo and Albert (2013), we can consider an expanded version of a given Boolean system by constructing negated variables. Each variable X_i in the original system has a corresponding negated variable $\overline{X}_i$ in the expanded system that is constrained to obey $\overline{X}_i = \neg X_i$, where $\neg$ is the Boolean "Not" operator. We then construct a network with all X_i and $\overline{X}_i$ as "virtual" nodes and with directed edges from a (regular or negated) node A to B whenever $B^*\big|_{A=1} \equiv 1$ (i.e., when $A = 1$ implies $B^* = 1$). In this network, all cycles that do not contain both a variable and its negation are so-called "stable motifs". (See Figure 1 for a brief example.) The simplified definition presented here is a special case of stable motif (also considered by Maheshwari and Albert (2017)), which we call a "cyclic stable motif" when discussing results that do not apply to the more general concept (see Zañudo and Albert (2013) for details). Stable motifs represent self-sustaining subsystems that are characterized by positive feedback among the variables involved in the motif and a steady state in which non-negated variables are "active" and negated variables are "inactive". The subsystem steady state persists independent of the states of other variables in the system. Therefore, stable motifs represent subsystems that cannot be externally controlled.

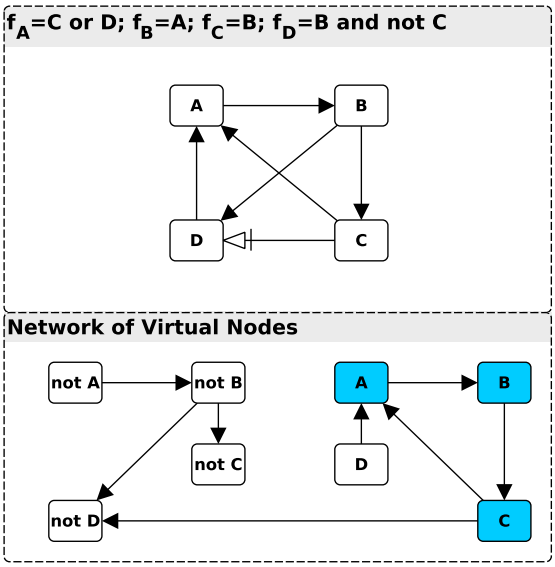

Figure 1: Example of a stable motif in a Boolean system. The top panel shows the network diagram and regulatory (update) functions for this system. Solid arrows represent activation, and the white barred arrow represents inhibition. In the bottom panel, the two states for each variable are represented as virtual nodes, with arrows representing sufficiency (e.g., $C = 1$ is sufficient for $D^* = 0$). The presence of the cycle ABC in the bottom panel implies that if A is active, then B will activate, which is sufficient to activate C, which can stabilize A. Because this cycle does not contain both a node and its negation, it is a cyclic stable motif that implies that the activity of the positive feedback loop ABC in the upper panel is self-sustaining.

3. Generalization to Continuous-Valued Systems

Gan and Albert (2018) generalize the concept of stable motifs to discrete multi-level systems, and Rozum and Albert (2018) discuss stable motifs in the context of more general dynamical systems. Here, we present a generalization of cyclic stable motifs that applies to monotonic ODEs constructed of Hill functions, which are of the form $H(x) = \frac{x^n}{x^n+k^n}$. Such ODEs are often used to model gene regulatory networks and signal transduction networks and are motivated by considering the kinetics of protein binding (Karlebach and Shamir, 2008; Mackey et al., 2016). These ODEs also have a close relationship with Boolean dynamics, and there are algorithmic approaches to converting Boolean systems into Hill function ODEs that preserve all Boolean steady states (Krumsiek et al., 2010; Wittmann et al., 2009). The prescription for such a transformation is to replace update rules $X_i^* = f_i(X_1, X_2, ..., X_N)$ with the derivative equation

$$\tau_i \dot{x}_i = \sum_{X_1=0}^{1} \sum_{X_2=0}^{1} ... \sum_{X_N=0}^{1} f_i(X_1, X_2, ..., X_N) \prod_{j=1}^{N} \left[H_{ij}(x_j) X_j + (1 - H_{ij}(x_j))(1 - X_j)\right] - x_i. \quad (1)$$

Here, each x_i is the real-valued analogue of the Boolean variable X_i, and decays at a constant rate $1/\tau_i$ if fully deactivated. Each Hill function, H_{ij}, in Equation 1 has independent parameters. Krumsiek et al. (2010) and Wittmann et al. (2009) motivate the form of Equation 1 by its correspondence with Boolean behavior and experimental results. We provide a kinetic motivation for this functional form in the Supporting Information.

We replace the notion of "active" versus "inactive" with that of being above or below certain thresholds, which are not specified a priori. For an ODE system $\dot{x}^i = R^i(\boldsymbol{x})$, we construct an expanded network with virtual nodes $x^i > T_H^i$ and $x^i < T_L^i$, and edges between nodes if the sustained truth of the parent statement implies that the child statement will become true in a finite time and remain true while the parent statement is true. We will have three tasks: 1) choose appropriate values for T_H^i and T_L^i, 2) identify when edges between virtual nodes are warranted, and 3) identify and interpret cycles that that do not have contradictory virtual nodes. The first two tasks are the most difficult and are inseparably linked, and so we approach these tasks for ODE systems of a particular form, as tabulated in Table 1. For instance, consider the ODE $\tau \dot{z} = \frac{x^n}{x^n+k^n} + \frac{y^n}{y^n+k^n} - \frac{y^n}{y^n+k^n}\frac{x^n}{x^n+k^n} + \alpha - z$. By identifying $F(x,y) = \frac{y^n}{y^n+k^n} - \frac{y^n}{y^n+k^n}\frac{x^n}{x^n+k^n} + \alpha$, which is bounded below by α, we can read from the table that an edge from virtual node $x > T_H^x$ to virtual node $z > T_H^z$ is present in the expanded network if T_H^z is no more than $\alpha + \frac{(T_H^x)^n}{(T_H^x)^n+k^n}$. This relationship between $x > T_H^x$ and $z > T_H^z$ holds regardless of the value of y. We have thus constructed one edge of the expanded network: the edge from $x > T_H^x$ to $z > \alpha + \frac{(T_H^x)^n}{(T_H^x)^n+k^n}$ which is a valid edge between nodes for any choice of T_H^x between zero and one.

The properties of Table 1 illustrate an important fact about the relationship between Boolean and continuous modeling. Observe that the effects of additional regulators, encapsulated in the functions F, are positive and bounded above by one (in the normalized scheme here). In practice, these additional regulatory

$x \implies z$		Boolean rule	ODE	F constraints
$> T_H^x$	$> T_H^z$	$z^* = x \vee ...$	$\tau \dot{z} = H_{n;k}(x) + F - z$	$F \geq T_H^z - H_{n;k}(T_H^x)$
$< T_L^x$	$> T_H^z$	$z^* = \overline{x} \vee ...$	$\tau \dot{z} = 1 - H_{n;k}(x) + F - z$	$F \geq T_H^z - 1 + H_{n;k}(T_L^x)$
$> T_H^x$	$< T_L^z$	$z^* = \overline{x} \wedge ...$	$\tau \dot{z} = (1 - H_{n;k}(x))F - z$	$F \leq \frac{T_L^x}{1 - H_{n;k}(T_H^z)}$
$< T_L^x$	$< T_L^z$	$z^* = x \wedge ...$	$\tau \dot{z} = H_{n;k}(x)F - z$	$F \leq \frac{T_L^x}{H_{n;k}(T_L^z)}$

Table 1: Variables above T_H are considered "active", while variables below T_L are "inactive". The first two columns indicate a relationship between two threshold statements that is analogous to the Boolean rule given in the third column. The ODE column specifies the form of the ODE in which the relationship is realized, with $F = F(\boldsymbol{x})$ an arbitrary function, subject to the constraints in the "F constraints" column. Note that these imply constraints on the thresholds in prototypical cases in which x is the only regulator of z (i.e., when $F(\boldsymbol{x})$ is zero or one). In all cases, $H_{n;k}(x) = \frac{x^n}{x^n + k^n}$ is a normalized Hill function.

functions, F, will not attain their extreme values. Therefore, the presence of additional regulators will tend to increase the activity of the "OR" rule ODEs (first two rows of Table 1), while decreasing the activity of the "AND" rule ODEs (last two rows of Table 1). In general, demanding agreement between Boolean models and continuous systems on the boundaries of state space causes the Boolean approximations to underestimate the activity of variables governed by "OR" rules and overestimate the activity of variables governed by "AND" rules.

By analogy with the Boolean concept, we call cycles consisting of compatible threshold statements "cyclic stable motifs" (Maheshwari and Albert, 2017; Zañudo and Albert, 2013). As in the Boolean case, cyclic stable motifs correspond to self-sustaining subsystems. These motif subsystems are associated with "trap spaces" given by the region in state space in which all cycle statements are true. Once the system trajectory enters this region, it cannot leave, even if variables outside the motif subsystem are externally manipulated.

Furthermore, motif subsystems are always positive feedback loops in the monotonic Hill function ODEs under consideration here, as we will now prove. There are two statement types $x^i > T_H^i$ (active type) and $x^i < T_L^i$ (inactive type). An edge between statements of the same type indicates an activating, or positive, effect between nodes in the motif subsystem; this is because there are initial conditions for which forcing the parent variable to cross its threshold causes the child variable to cross its threshold from the same direction. Similarly, edges between statements of different types correspond to an inhibitory effect of the parent variable on the child variable. We may divide the statement cycle into maximally long sequences of nodes of the same type. In following the cycle from an arbitrary starting node, we may enter a region of different type, indicating an inhibitory effect, and an additional inhibitory effect is indicated upon exiting that region. Because the cycle ends on the starting node, we must exit every region of different statement type that we enter. Therefore, there is an even number of inhibitory effects in the motif subsystem cycle, i.e., the motif subsystem is a positive feedback loop.

This result indicates a close relationship between control-robust, self-sustaining subsystems and positive feedback loops. Furthermore, it allows us to prescribe a search procedure for identifying cyclic stable motifs. We search the system for positive feedback loops in which each regulatory relationship is of one of the forms tabulated in Table 1. By inspection, we can place lower or upper bounds on the "F" functions in Table 1 because each Hill function is bounded. This results in a system of inequalities in the thresholds. These inequalities can be written in the form $0 \leq G_i\left(T^i, T^{i+1}\right)$ for each variable in the positive feedback loop (where T^i is the upper or lower threshold for the variable x^i). By iteratively composing these inequalities, we can eliminate all but any one variable threshold, T, which gives an inequality $0 \leq \mathscr{G}(T)$. Solving this inequality (perhaps numerically) and then back substituting gives the thresholds for all variables in the cycle.

This procedure is closely related to a special case of the monotone system techniques of Angeli et al. (2004) and Angeli and Sontag (2004); here, rather than identify steady states, we find trap spaces in the dynamics. This is a weaker restriction on the dynamics, but it can be achieved in cases when the methods of Angeli et al. (2004) and Angeli and Sontag (2004) do not apply. Namely, our approach applies even when variables in a positive feedback loop have additional mediators that introduce negative feedback loops or incoherent feed forward loops. Furthermore, our methods are still applicable when parameter values are uncertain (but bounded). By incorporating the parameter bounds as additional inequalities in the system of inequalities to be solved, solutions for thresholds will correspond to cyclic stable motifs that are valid throughout the parameter space. This approach has the computational benefit of examining small subsystems at the boundaries of parameter space, rather than requiring integration of the entire system for each combination of parameters. The computational time is determined primarily by the number of positive feedback loops and the desired precision of the virtual node bounds.

4. Example Applications

In this section, we present several prototypical subnetworks common to gene regulatory networks. We analyze these examples, within our framework presented above, to illustrate its utility in the study of multistability, hysteresis, signal cross-talk (feedforward loops), and system control.

4.1. Simple feedback loop and multistability

We consider the multistability of a simple gene regulatory feedback loop (Figure 2A):

$$\begin{aligned} \tau_x \dot{x} &= \frac{y^{n_x}}{y^{n_x} + k_x^{n_x}} - x \equiv H_x(y) - x \\ \tau_y \dot{y} &= \frac{x^{n_y}}{x^{n_y} + k_y^{n_y}} - y \equiv H_y(x) - y. \end{aligned} \tag{2}$$

To do this, we ask whether x and y can be maintained above as-of-yet unspecified thresholds, $x > T_H^x$

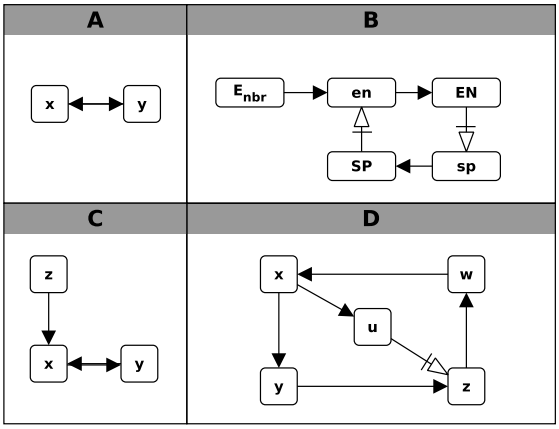

Figure 2: Network structures representing prototypical ODEs common in gene regulatory networks. In panel A, we present the topology of Equations 2. In panel B, we depict the topology of Equations 4. In panel C, we present the shared topology of Equations 5 and 6. Panel D depicts the topology of Equations 7. In all panels, solid black arrows represent positive regulation, and the white barred arrows represent inhibition.

and $y > T_H^y$. This would require the following to hold:

$$\begin{aligned} T_H^x &\leq H_x\left(T_H^y\right) \\ T_H^y &\leq H_y\left(T_H^x\right). \end{aligned} \tag{3}$$

Composing these gives $T_H^x \leq H_x\left(T_H^y\right) \leq H_x\left(H_y\left(T_H^x\right)\right)$. The marginal case, $0 = H_x\left(H_y\left(T_{Hx}\right)\right) - T_{Hx}$, can be solved numerically or graphically. Similarly, we can determine whether x and y can be maintained below thresholds, $x < T_L^x$ and $y > T_L^y$. By the same argument, this requires $T_L^x \geq H_x\left(H_y\left(T_L^x\right)\right)$. Thus, the existence of multiple roots of $H_x\left(H_y\left(T\right)\right) - T$ on the interval $(0, 1)$ indicates multistability.

4.2. Mutual Inhibition in Establishing Drosophila Segment Polarity

To illustrate the method in the case of mutual inhibition in a model from the literature, we consider the *sloppy-paired/engrailed* feedback loop of the *Drosophila melanogaster* segment polarity network, as modeled by Ingolia (2004). The full model describes the gene regulation underlying the formation of embryonic segments in *Drosophila*, and this feedback loop is modulated by the averaged saturation fraction of extracellular *wingless* protein on neighboring cells ($[E_{nbr}]$). We have previously conducted an analysis of the full network (Rozum and Albert, 2018); here we focus on one feedback loop in particular (shown in Figure 2B), and especially on how it responds to the level of expression of *wingless* in the neighboring cells. The subsystem we will study here is given in Equations 4.

$$\begin{aligned}
\frac{d[en]}{dt} &= H([E_{nbr}])(1 - H([SP])) - [en] \\
\frac{d[EN]}{dt} &= [en] - [EN] \\
\frac{d[sp]}{dt} &= 1 - H([EN]) - [sp] \\
\frac{d[SP]}{dt} &= [sp] - [SP], \qquad (4)
\end{aligned}$$

where H is the Hill function defined by $H(x) = \frac{x^2}{x^2+1/16}$. Capitalized variables represent *engrailed* ($[EN]$) and *sloppy-paired* ($[SP]$) protein saturation fractions, and lower case variables ($[en]$ and $[sp]$) represent the corresponding mRNA saturation fractions. We have chosen parameters arbitrarily within the biologically plausible region. To begin our analysis, we assume that $[E_{nbr}]$ is fixed (i.e., the neighboring cells are in a steady state). We will relax this assumption when we apply our new methods to analyze the system.

The system is the closure of a monotone system (i.e., it has no incoherent feedforward or negative feedback loops). We leverage this fact to apply traditional approaches in addition to our less precise, but more general methods to study the effect of varying the input parameter $[E_{nbr}]$ on the steady states of the system. Note that any steady state of the system is uniquely determined by the steady state value of any of the four variables (e.g., if the system is at steady state with $[sp] = x$, then it follows that $[SP]$ must take the value x as well, and further that $H([E_{nbr}])(1 - H(x))$ is the steady state value of both $[en]$ and $[EN]$). Therefore, we can characterize the steady states of the system by the steady state values of $[sp]$. Furthermore, by applying theorem 3 of Angeli and Sontag (2004), we can identify all such steady states and determine their stability by considering the roots of the function $\kappa([sp]) = H([E_{nbr}])(1 - H([sp])) - [sp]$ for any fixed $[E_{nbr}]$. The slope of $\kappa([sp])$ at any of its roots determines the stability of the steady state: negative slope implies stability, positive slope implies instability. We numerically construct the bifurcation diagram of Figure 3, which shows that a low value of $[sp]$ can only be maintained at steady state for sufficiently high value of $[E_{nbr}]$, larger than about 0.5125. In addition, our analysis reveals that the steady states with the lowest and highest values of $[sp]$ are stable. Thus the system is monostable when $[E_{nbr}]$ is below 0.5125, and bistable above this value.

Next, we expand upon the classical analysis of Equations 4 using the concept of cyclic stable motifs to determine what information about the system generalizes to the case in which $[E_{nbr}]$ is not held fixed.

We translate the regulatory functions of Equations 4 into causal relationships between virtual nodes. For example, if $[en]$ is less than or greater than some threshold for sufficiently long, this will drive $[EN]$ above or below the same threshold. In the language of virtual nodes, this statement implies that any virtual node $[en] \lessgtr T$ has an edge to $[EN] \lessgtr T$ in the expanded network. The same argument applies to $[sp]$ and $[SP]$. Furthermore, note that $[EN]$ inhibits $[sp]$, and $[SP]$ inhibits $[en]$. It is therefore reasonable to guess that cyclic stable motifs of the forms $[en] \lessgtr T_1 \to [EN] \lessgtr T_1 \to [sp] \gtrless T_2 \to [SP] \gtrless T_2$ might exist. Note that the direction of the inequalities is opposite for the *sloppy-paired* variables as compared to the *engrailed* variables;

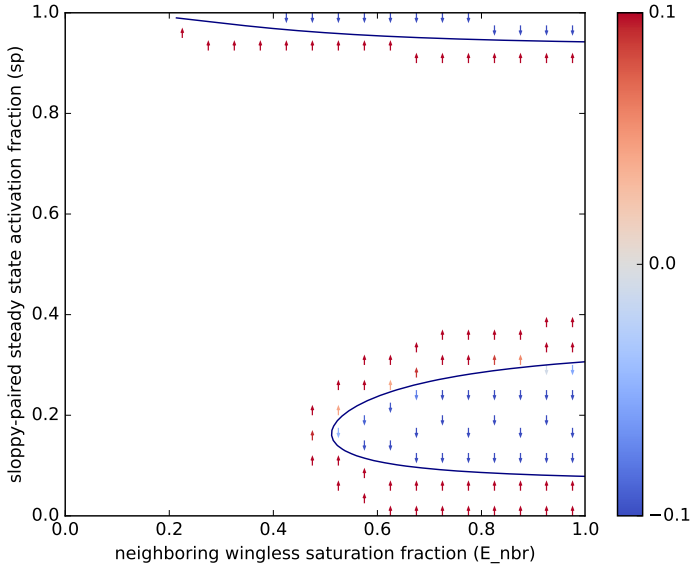

Figure 3: Bifurcation diagram of the system given in Equations 4. The solid lines correspond to the steady state values of $[sp]$ for any fixed value of $[E_{nbr}]$. The vector field is given by $\kappa([sp]) = H([E_{nbr}])(1 - H([sp])) - [sp]$ in the $[sp]$ direction. The vector field provides a qualitative representation of the steady state stability, but not necessarily of the actual system trajectories, as these depend upon the initial values of the other three system variables (Angeli and Sontag, 2004).

this is a general feature of cyclic stable motifs supported by mutual inhibition feedback loops.

We consider that $[E_{nbr}]$ varies between 51.25% and 100% of its maximum value, one. Biologically, this corresponds to the case in which neighboring cells are expressing *wingless*, but the precise expression level varies, perhaps stochastically. Mathematically, this interval corresponds to the region of bistability in the case of constant $[E_{nbr}]$, as represented in Figure 3. We can analyze this case by considering the "worst-case" system for each of our two candidate cyclic stable motifs (one candidate has $[en] > T_1$ and $[sp] < T_2$, while the other has the inequalities reversed). The construction of the worst-case sytem relies on the observation that an increase (decrease) in $[E_{nbr}]$ results in an increase (decrease) of $[en]$ and $[EN]$, while decreasing (increasing) $[sp]$ and $[SP]$.

In one cyclic stable motif candidate, $[sp]$ is bounded below while $[en]$ is bounded above. A decrease in $[E_{nbr}]$ perturbs $[sp]$ and $[en]$ toward violation of these bounds. Therefore, the worst-case system for the first candidate cyclic stable motif is characterized by $\frac{d[en]}{dt} = H\left(0.5125\right)\left(1 - H\left([SP]\right)\right) - [en]$ (and the other equations as in Equations 4). The steady state of this worst-case system with the lowest value of $[sp]$ (and thus the highest value of $[en]$) is given by $[sp] = [SP] \approx 0.16$ and $[en] = [EN] \approx 0.58$. Therefore, one cyclic stable motif for this system is $[sp] < 0.16 \rightarrow [SP] < 0.16 \rightarrow [en] > 0.58 \rightarrow [EN] > 0.58$. Note that this corresponds to the uppermost solid line of Figure 3 at $[E_{nbr}] = 0.5125$. In the other candidate stable motif, $[sp]$ is bounded below and $[en]$ is bounded above. In this case, the worst-case system is characterized by a fixed large value of $[E_{nbr}]$, i.e., we set $[E_{nbr}]$ to its maximum value, one. We then find the cyclic stable motif $[sp] > 0.96 \rightarrow [SP] > 0.96 \rightarrow [en] < 0.052 \rightarrow [EN] < 0.052$ from the steady state of this worst-case system with the largest value of $[sp]$ (and thus lowest value of $[en]$). These two cyclic stable motifs describe positive invariant sets (i.e., trap spaces) that are valid for as long as $[E_{nbr}]$ remains in the interval $[0.5125, 1]$. We may uncover less restrictive (i.e., bigger) trap spaces by considering the other steady states of the two worst-case systems we have already constructed; any steady state of a worst case system provides valid bounds for a candidate cyclic stable motif.

4.3. Hysteresis

Hysteresis has been extensively studied in biological models and captures the tendency for the effects of a process to persist after the process is reversed (e.g., Angeli et al., 2004; Laslo et al., 2006; Robeva and Murrugarra, 2016). Because hysteresis often occurs when one steady state transitions into another, it is tightly linked to multistability, and therefore to positive feedback loops. We consider this relationship by applying our method of cyclic stable motifs in two toy examples of gene regulatory networks.

In both examples, we consider a gene, x, positively regulated by genes y and z. We suppose that x up-regulates y and that z is regulated by some upstream or external processes that we will not explicitly consider. The two examples differ in the nature of the cooperation between y and z and will serve to highlight the benefit of applying Boolean reasoning to continuous models.

In our first example, we consider the following model (Figure 2C):

$$\begin{aligned}\dot{x} &= \frac{z^4 y^3}{\left(z^4+1/2^4\right)\left(y^3+1/2^3\right)} - x \\ \dot{y} &= \frac{x^3}{x^3+1/2^3} - y. \end{aligned} \tag{5}$$

When z is saturated ($z(t) \equiv 1$), we observe that x and y are potentially involved in cyclic stable motifs $x \gtrless T^x \rightarrow y \gtrless T^y = \frac{(T^x)^3}{(T^x)^3+1/8}$. Indeed, by composing inequalities, we find that $T_H^x \approx 0.73$ and $T_L^x \approx 0.53$ are valid thresholds for x, while $T_H^y \approx 0.76$ and $T_L^y \approx 0.54$ are valid thresholds for y. In this simple example, these thresholds correspond to the two steady states of the system, but by interpreting these inequalities as Boolean statements regarding the "worst-case" system behavior, we can gain deeper insight into the controllability of the system. For example, decreasing z will always serve to decrease x and, eventually, y; specifically, when z is absent, x will approach zero and so too will y. If $x < T_L^x$ and $y < T_L^y$ both hold at any given time, then they will continue to hold forever, regardless of the value z takes (provided z remains less than its saturation value of one). We can interpret this to mean that low values of x and y are self-maintaining and the regulatory effect of z on x is insufficient to overcome this self-sustained inactivity.

To see the impact of this observation, consider x, y, and z initially at their saturation levels, and let z be maintained at $z = 1$. Then x and y will approach their upper thresholds $T_H^x \approx 0.73$ and $T_H^y \approx 0.76$. If z is then removed (perhaps due to a loss-of-function mutation), x and y will approach zero. If the system is later rescued (e.g., by ectopic expression of z) then x and y, being below their low thresholds, remain below $T_L^x \approx 0.53$ and $T_L^y \approx 0.54$, respectively. This upper bound on x and y remains enforced even if z is held at its saturation value of one.

In the above example, genes y and z were both required for activation of x; now we consider the case in which either gene is sufficient to activate x (Figure 2C):

$$\begin{aligned}\dot{x} &= \frac{y^2 z^2 + y^2/4 + z^2/4}{y^2 z^2 + y^2/4 + z^2/4 + 1/16} - x \\ \dot{y} &= \frac{x}{x+1/2} - y. \end{aligned} \tag{6}$$

As before, we consider the cases in which $z(t) \equiv 1$ or z is fully absent ($z(t) \equiv 0$). In the latter case, we find $\dot{x} = \frac{y^2}{y^2+1/4} - x$ and $y = \frac{x}{x+1/2} - y$. By considering $T \gtrless \left(\frac{T}{T+1/2}\right)^2 / \left(\left(\frac{T}{T+1/2}\right)^2 + 1/4\right)$, we see that $x \gtrless \frac{1}{2} \rightarrow y \gtrless \frac{1}{2} \rightarrow x \gtrless \frac{1}{2}$ holds in this case, as does $x \gtrless \frac{1}{10} \rightarrow y \gtrless \frac{1}{6} \rightarrow x \gtrless \frac{1}{10}$. When $z = 1$, however, $\dot{x}$ becomes $\dot{x} = \frac{y^2+1/5}{y^2+1/4} - x$, and thresholds can be found as before by considering $T \gtrless \left(\left(\frac{T}{T+1/2}\right)^2 + 1/5\right) / \left(\left(\frac{T}{T+1/2}\right)^2 + 1/4\right)$. Now there is only one solution, $x \gtrless 0.93 \rightarrow y \gtrless 0.65$.

These threshold values are merely the steady states of the system for particular fixed values of z. Nevertheless, because we have considered extremal values of z, we are provided with an interpretation that holds for all values of z. Because an increase in z will increase x and y, the lower bounds in the $z = 0$ case are valid for all values of z. In particular, if $x, y > 1/2$ holds at any time, then it holds for all times.

To put this in the context of hysteresis, we consider that x and y determine the rate of cell proliferation, and high, uncontrolled proliferation is an abnormal state such as that of cancer cells. The system has a "healthy", non-proliferative state in which x, y, and z are suppressed ($x < \frac{1}{10}$, $y < \frac{1}{6}$, $z = 0$) and a "disease" state in which z is fully active, driving x and y toward the expression levels 0.93 and 0.65, respectively, corresponding to uncontrolled cell proliferation. Knowing that over-expression of z is the cause of the disease state, one might attempt to treat the disease by suppressing z. However, because x and y have been driven above the values $x = y = 1/2$, they are trapped in that region of state-space, independent of z. Therefore, even complete elimination of z can only achieve a modest reduction in the over-expression of x and y, which remain expressed at levels several times greater than their "healthy" values, maintaining an unhealthy level of cell proliferation.

4.4. Effects of Cross-Talk and External Control

In more complex systems, incoherent feedforward (cross-talk) complicates the process of identifying steady states by recursively composing the steady state equations of each variable. Further complications arise in the presence of oscillations or noise, which might eliminate steady states. Nevertheless, positive feedback loops can still sustain trap spaces and cyclic stable motifs may still exist. We illustrate this point first with a toy example, and then in the T-cell signal transduction network model used in Wittmann et al. (2009).

4.4.1. A Prototype for Ignored Cross-Talk and Ineffective Therapy

We will consider a gene regulatory system in which four genes, w, x, y, and z participate in a positive feedback loop (Equation 7). The expression of z is also inhibited by a fifth gene, u, which is activated by x. Thus, the system consists of intersecting positive (w, x, y, z) and negative (x, u, z, w) feedback loops (Figure 2D). We choose a simple first approximation for this system in which the evolution of each variable is described by Hill functions and parameters are chosen for convenience (but within biologically relevant ranges):

$$\begin{aligned} \dot{w} &= H(z) - w \\ \dot{x} &= H(w) - x \\ \dot{y} &= H(x) - y \\ \dot{u} &= H(x) - u \\ \dot{z} &= 1 - H(u)\,(1 - H(y)) - z \\ H(\cdot) &= \frac{[\cdot]^2}{[\cdot]^2 + 1/4}. \end{aligned} \tag{7}$$

We are interested in whether or not the positive feedback loop can maintain the activity of its members despite the inhibitory effect of u on z.

To answer our hypothetical question, consider the positive feedback loop (w, x, y, z) and the case in which these genes are simultaneously active. If there is a cyclic stable motif for this feedback in which the genes are active, it must take the following form:

$$(w > T_w) \to (x > T_x) \to (y > T_y) \to (z > T_z) \to (w > T_w)\,. \tag{8}$$

The inhibition of z by u means that we cannot simply solve a steady state equation as we have done in previous examples. Nevertheless, we may consider a "worst-case" effect of u on z to determine whether or not the positive feedback loop is able to sustain the system behavior. The variable u will not attain values larger than one if the system evolves without intervention. If u is externally manipulated, however, it may become quite large. Because we do not know in advance how large u can be made, we consider that it might be driven to arbitrarily large values. Because the response of z to u saturates, this does not allow the rest of the system to diverge, and simplifies the calculations to follow. Thus, we take our "worst-case" value of u to be infinity. These considerations lead to the following system of inequalities:

$$\begin{aligned} T_w &\leq H\left(T_z\right) \\ T_x &\leq H\left(T_w\right) \\ T_y &\leq H\left(T_x\right) \\ T_z &\leq 1 - H\left(\infty\right)\left(1 - H\left(y\right)\right) = H\left(y\right). \end{aligned} \tag{9}$$

This system of inequalities has the marginal solution $T_w = T_x = T_y = T_z = \frac{1}{2}$. We interpret this result as follows. If $w, x, y, z > \frac{1}{2}$ holds at any time, then it will continue to hold for all time, even if u is externally controlled. This means that the effect of the cross-talk mediated by u is bounded, and can never disrupt activity above 50% in the feedback loop.

To further illustrate the implications of this observation, consider that activation of a gene, v, is associated with some disease and governed by

$$\dot{v} = \frac{w^4}{w^4 + (1/4)^4} - v. \tag{10}$$

We are interested in the prospect of using the product of u as a drug to be delivered in order to disrupt the expression of v via the regulatory pathway through z and w. We consider our goal accomplished if the activation fraction of v is below 50%. However, we have seen that arbitrary manipulations of u are insufficient to decrease the activation fraction w below 50% once the (w, x, y, z) feedback loop has become active. If w is above 1/2, then the activation fraction of v will eventually become and remain larger than $\frac{(1/2)^4}{(1/2)^4+(1/4)^4} \approx 0.94$. The implication is that the effectiveness of u as a therapeutic option is extremely limited.

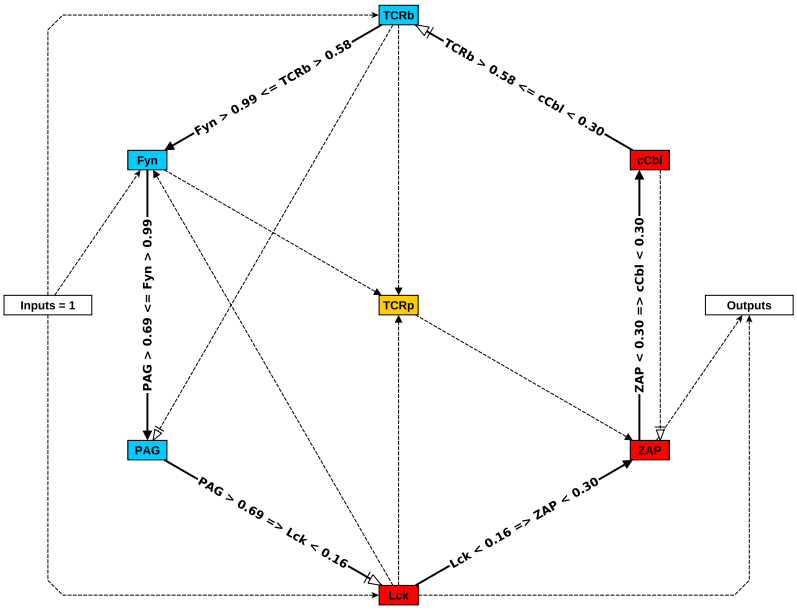

Figure 4: Network representation of the T-cell signal transduction network model of Wittmann et al. (2009). Black arrows represent activation, and white arrows represent inhibition. Bold, labeled edges represent regulatory effects that contribute to the cyclic stable motif that is indicated by the edge labels. Dotted lines represent regulatory effects that do not participate in the cyclic stable motif. The cyclic stable motif edges (bold) form a positive cycle, as we have proved must be the case. Blue nodes (TCRb, Fyn, PAG) are maintained above thresholds in the cyclic stable motif, while red nodes (Lck, ZAP, cCbl) are maintained below thresholds. The yellow node (TCRp) is the only member of the network core that does not participate in the cyclic stable motif. As such, external manipulation of this variable is insufficient to disrupt the behavior characterized by the cyclic stable motif.

4.4.2. T-Cell Signaling Network Example

To illustrate how cross-talk can be ignored in real systems, we consider the T-cell signal transduction network model of Wittmann et al. (2009). This model describes how T-cells process signals from external ligands binding to receptors. This ODE model is also interesting to consider because it represents an explicit attempt to replicate the behavior of a Boolean model, allowing us to compare the stable motif results for the two modeling approaches. For simplicity, we consider the case of high input signals and we disregard biomolecules downstream of the strongly connected core of the system, as these do not play a role in determining the system dynamics. The resulting system is depicted in Figure 4.

To search for cyclic stable motifs, we first identify the positive feedback in the system. We focus on the positive feedback loop $(TCRb, Fyn, PAG, Lck, ZAP, cCbl)$. We can then attempt to identify thresholds such that $TCRb > T_H^{TCRb} \rightarrow Fyn > T_H^{Fyn} \rightarrow ... \rightarrow cCbl < T_L^{cCbl} \rightarrow TCRb > T_H^{TCRb}$ is a cyclic stable motif. We treat each threshold pair in isolation, so that when considering, for example, $TCRb > T_H^{TCRb} \rightarrow Fyn > T_H^{Fyn}$, we do not assume anything about the value of Lck, which also activates Fyn. Therefore, T_H^{TCRb} must be large enough that $TCRb > T_H^{TCRb} \rightarrow Fyn > T_H^{Fyn}$ holds even when Lck is as small as possible ($Lck = 0$). Similarly,

because PAG is activated by Fyn and inhibited by $TCRb$, $Fyn > T_H^{Fyn} \rightarrow PAG > T_H^{PAG}$ must hold even when $TCRb$ is maximal ($TCRb = 1$). Considering each relationship in this pairwise and independent manner yields a system of inequalities that can be solved by composition. The resulting solution is depicted along the network edges in Figure 4. Note that this result is in agreement with Schwieger et al. (2018), who have identified an analogous trap space in this ODE model by considering the relationship between the Boolean and ODE models of Wittmann et al. (2009). Our method does not rely on any associated Boolean model for the ODEs under consideration.

Note that all variables are constrained by the cyclic stable motif except for $TCRp$. We interpret this to mean that the cyclic stable motif conditions are maintained independent of $TCRp$. Indeed, numerical simulations support this conclusion and demonstrate that the system threshold behavior cannot be altered by external manipulation of $TCRp$ (Rozum and Albert, 2018). Instead, direct disruption of the constrained variables is required to disrupt their collective behavior.

We can compare the ODE model considered above to its Boolean counterpart (Wittmann et al., 2009) using the stable motif methods of Zañudo and Albert (2013). If we examine the same feedback loop we have considered above (but now in the Boolean system), we see that each variable in the cycle (or its negation) is sufficient for activation or deactivation of the next, i.e., $Fyn = 1$ is sufficient for $PAG = 1$, which is sufficient for $Lck = 0$, which is sufficient for $ZAP = 0$, and so on. This pattern is such that the configuration in which $TCRb = Fyn = PAG = 1$ and $Lck = ZAP = cCbl = 0$ is stable and independent of the value of $TCRp$, in analogy with the result we have presented above for the ODE model. This highlights the important fact that positive feedback in discrete and continuous systems can be analyzed in a similar manner.

5. Discussion

We have shown that cyclic relationships between comparisons of Hill functions to their arguments allows for the identification of cyclic stable motifs, a concept analogous to the stable motifs of discrete systems introduced by Zañudo and Albert (2013) and generalized by Gan and Albert (2018). Cyclic stable motifs are subsystems with an associated region of state space that is a "trap space" for the subsystem, i.e., once the subsystem enters this region of state space, it does not leave. A cyclic stable motif is constructed in such a way that this property holds regardless of the values of variables not in the subsystem, allowing for the identification of control-robust behavior of subsystems, such as stability with respect to specified thresholds. Our notion of cyclic stable motifs is closely related to the concept of feedback loop characteristic states (Snoussi and Thomas, 1993), but with emphasis placed upon identification of explicit variable thresholds that characterize system trap spaces.

Using our approach, we have analyzed prototypical gene regulatory models exhibiting hysteresis, bistability, and control robustness (resistance to therapeutic intervention). We have also analyzed the T-cell signal transduction network model of Wittmann et al. (2009) (which is further explored by Rozum and Albert

(2018)). We have also compared our method of cyclic stable motifs to traditional techniques in the analysis of mutual inhibition in the *Drosophila* segment polarity gene network model of Ingolia (2004) (Equations 4). We comment that traditional visual methods, such as phase portraits and bifurcation diagrams (in the spirit of Figure 3) become cumbersome as the system dimension becomes large. In this example, we were able to leverage powerful properties of monotone systems (using results of Angeli and Sontag (2004)) to enable visualization of this five-dimensional system in a two-dimensional figure. Many biological systems, however, are not amenable to such a simplification. The crux of the method of cyclic stable motifs is to identify a "worst-case" subsystem that can be analyzed using these simplifications, and to pick out properties of the worst-case subsystem that are preserved within the real system. In this way, we can study a large, complex system by bounding the behavior of its simpler constituent subsystems.

In all examples considered here, cyclic stable motifs have characterized the roles of positive feedback loops in the system. This is not a coincidence, and indeed we have proved that cyclic stable motifs always arise from positive feedback loops, as is the case for Boolean and other discrete dynamical systems (Gan and Albert, 2018; Zañudo and Albert, 2013). The complexity of identifying cyclic stable motifs in a system depends primarily upon the difficulty of finding positive feedback loops in the regulatory graph, a task for which fast software implementations are already developed. Determining whether or not a given positive feedback loop supports a cyclic stable motif involves holding additional regulatory effects constant and numerically finding the root of a function constructed by composing regulatory functions; the complexity of this process scales linearly with the number of variables in the feedback loop. Furthermore, the methods described here need not be applied to an entire system; the additional regulation functions (F in Table 1) can be of arbitrary form. Thus, even in situations in which our methods are not generally applicable, they may still be used to glean useful information about key subsystems.

Our results illustrate the important insights about positive feedback loops in biological systems put forth by René Thomas and his colleagues (Glass and Kauffman, 1973; Snoussi and Thomas, 1993; Thomas and Kaufman, 2001a,b). Building upon these paradigms, investigators of biological systems have increasingly highlighted the fundamental role of feedback in determining dynamical repertoires (Albert and Othmer, 2003; Angeli et al., 2004; van Dassow, G. et al., 2000; Wittmann et al., 2009; Yao et al., 2014). For example, Shinar and Feinberg (2010) relate feedback loops in mass action networks to maintained values of individual variables. Our main result is analogous; while Shinar and Feinberg (2010) consider the maintained truth of an equality statement about a variable, we consider the maintained truth of inequalities about multiple variables. Snoussi and Thomas (1993) have previously shown the utility of a logical framework for the analysis of ODE systems. Here, we have extended this notion by applying our recent generalization (Rozum and Albert, 2018) of techniques developed for discrete dynamical systems (Gan and Albert, 2018; Zañudo and Albert, 2013). The concept of a cyclic stable motif represents an explicit connection between Boolean and ODE systems, in the spirit of Snoussi and Thomas (1993). We have shown that such connections can

provide a conceptual framework for studying hysteresis and multistability in biomolecular circuits.

Acknowledgments

This work was funded by NSF grants PHY 1205840 and PHY 1545832 to RA. We thank Dr. Jorge Zaudo for his helpful insights and conversations.

References

Albert, R., Othmer, H. G., Jul. 2003. The topology of the regulatory interactions predicts the expression pattern of the segment polarity genes in Drosophila melanogaster. Journal of Theoretical Biology 223 (1), 1–18.
URL http://linkinghub.elsevier.com/retrieve/pii/S0022519303000353

Alves, B. N., Tsui, R., Almaden, J., Shokhirev, M. N., Davis-Turak, J., Fujimoto, J., Birnbaum, H., Ponomarenko, J., Hoffmann, A., Apr. 2014. IκBε Is a Key Regulator of B Cell Expansion by Providing Negative Feedback on cRel and RelA in a Stimulus-Specific Manner. The Journal of Immunology 192 (7), 3121–3132.
URL http://www.jimmunol.org/content/192/7/3121

Angeli, D., Ferrell, J. E., Sontag, E. D., 2004. Detection of multistability, bifurcations, and hysteresis in a large class of biological positive-feedback systems. Proceedings of the National Academy of Sciences 101 (7), 1822–1827.

Angeli, D., Sontag, E. D., Mar. 2004. Multi-stability in monotone input/output systems. Systems & Control Letters 51 (3-4), 185–202.
URL http://linkinghub.elsevier.com/retrieve/pii/S0167691103002317

Azpeitia, E., Muñoz, S., González-Tokman, D., Martínez-Sánchez, M. E., Weinstein, N., Naldi, A., Álvarez-Buylla, E. R., Rosenblueth, D. A., Mendoza, L., Feb. 2017. The combination of the functionalities of feedback circuits is determinant for the attractors' number and size in pathway-like Boolean networks. Scientific Reports 7, 42023.
URL https://www.nature.com/articles/srep42023

Bhalla, U. S., Iyengar, R., Jan. 1999. Emergent Properties of Networks of Biological Signaling Pathways. Science 283 (5400), 381–387.
URL http://science.sciencemag.org/content/283/5400/381

Collombet, S., Oevelen, C. v., Ortega, J. L. S., Abou-Jaoudé, W., Stefano, B. D., Thomas-Chollier, M., Graf, T., Thieffry, D., Jun. 2017. Logical modeling of lymphoid and myeloid cell specification and transdifferentiation. PNAS 114 (23), 5792–5799.
URL http://www.pnas.org/content/114/23/5792

Craciun, G., Feinberg, M., Jan. 2006. Multiple Equilibria in Complex Chemical Reaction Networks: II. The Species-Reaction Graph. SIAM J. Appl. Math. 66 (4), 1321–1338.
URL http://epubs.siam.org/doi/abs/10.1137/050634177

Fiedler, B., Mochizuki, A., Kurosawa, G., Saito, D., Sep. 2013. Dynamics and Control at Feedback Vertex Sets. I: Informative and Determining Nodes in Regulatory Networks. J Dyn Diff Equat 25 (3), 563–604.
URL https://link.springer.com/article/10.1007/s10884-013-9312-7

Gan, X., Albert, R., Apr. 2018. General method to find the attractors of discrete dynamic models of biological systems. Phys. Rev. E 97 (4), 042308.
URL https://link.aps.org/doi/10.1103/PhysRevE.97.042308

Glass, L., Kauffman, S. A., Apr. 1973. The logical analysis of continuous, non-linear biochemical control networks. Journal of Theoretical Biology 39 (1), 103–129.
URL http://www.sciencedirect.com/science/article/pii/0022519373902087

Ingolia, N. T., 2004. Topology and robustness in the Drosophila segment polarity network. PLoS Biology 2 (6), e123.

Karlebach, G., Shamir, R., Oct. 2008. Modelling and analysis of gene regulatory networks. Nature Reviews Molecular Cell Biology 9 (10), 770–780.
URL http://www.nature.com/doifinder/10.1038/nrm2503

Krumsiek, J., Pölsterl, S., Wittmann, D. M., Theis, F. J., 2010. Odefy-from discrete to continuous models. BMC bioinformatics 11 (1), 233.

Laslo, P., Spooner, C. J., Warmflash, A., Lancki, D. W., Lee, H.-J., Sciammas, R., Gantner, B. N., Dinner, A. R., Singh, H., Aug. 2006. Multilineage Transcriptional Priming and Determination of Alternate Hematopoietic Cell Fates. Cell 126 (4), 755–766.
URL http://www.sciencedirect.com/science/article/pii/S0092867406009809

Mackey, M. C., Santillán, M., Tyran-Kamińska, M., Zeron, E. S., 2016. Simple Mathematical Models of Gene Regulatory Dynamics. Lecture Notes on Mathematical Modelling in the Life Sciences. Springer International Publishing, Cham.
URL http://link.springer.com/10.1007/978-3-319-45318-7

Maheshwari, P., Albert, R., Dec. 2017. A framework to find the logic backbone of a biological network. BMC Systems Biology 11, 122.
URL https://doi.org/10.1186/s12918-017-0482-5

Mochizuki, A., Fiedler, B., Kurosawa, G., Saito, D., Oct. 2013. Dynamics and control at feedback vertex sets. II: A faithful monitor to determine the diversity of molecular activities in regulatory networks. Journal of

Theoretical Biology 335, 130–146.
URL http://linkinghub.elsevier.com/retrieve/pii/S0022519313002816

Pfeuty, B., Kaneko, K., Nov. 2009. The combination of positive and negative feedback loops confers exquisite flexibility to biochemical switches. Physical Biology 6 (4), 046013.
URL http://iopscience.iop.org/article/10.1088/1478-3975/6/4/046013/meta

Robeva, R., Murrugarra, D., Jan. 2016. The spruce budworm and forest: a qualitative comparison of ODE and Boolean models. Letters in Biomathematics 3 (1), 75–92.
URL https://www.tandfonline.com/doi/full/10.1080/23737867.2016.1197804

Rozum, J. C., Albert, R., Apr. 2018. Identifying controllable and uncontrollable dynamical behavior in complex networks. bioRxiv, 236323.
URL https://www.biorxiv.org/content/early/2018/04/05/236323

Schwieger, R., Siebert, H., Röblitz, S., Jan. 2018. Correspondence of Trap Spaces in Different Models of Bioregulatory Networks. SIAM J. Appl. Dyn. Syst. 17 (2), 1742–1765.
URL https://epubs.siam.org/doi/abs/10.1137/17M1155302

Shinar, G., Feinberg, M., Mar. 2010. Structural Sources of Robustness in Biochemical Reaction Networks. Science 327 (5971), 1389–1391.
URL http://science.sciencemag.org/content/327/5971/1389

Snoussi, E. H., Thomas, R., 1993. Logical identification of all steady states: the concept of feedback loop characteristic states. Bulletin of Mathematical Biology 55 (5), 973–991.

Steinway, S. N., Zañudo, J. G. T., Ding, W., Rountree, C. B., Feith, D. J., Loughran, T. P., Albert, R., Nov. 2014. Network Modeling of TGFβ Signaling in Hepatocellular Carcinoma Epithelial-to-Mesenchymal Transition Reveals Joint Sonic Hedgehog and Wnt Pathway Activation. Cancer Res 74 (21), 5963–5977.
URL http://cancerres.aacrjournals.org/content/74/21/5963

Thomas, R., Kaufman, M., Mar. 2001a. Multistationarity, the basis of cell differentiation and memory. I. Structural conditions of multistationarity and other nontrivial behavior. Chaos 11 (1), 170–179.
URL http://aip.scitation.org/doi/abs/10.1063/1.1350439

Thomas, R., Kaufman, M., Mar. 2001b. Multistationarity, the basis of cell differentiation and memory. II. Logical analysis of regulatory networks in terms of feedback circuits. Chaos 11 (1), 180–195.
URL http://aip.scitation.org/doi/abs/10.1063/1.1349893

Tian, X.-J., Zhang, H., Xing, J., Aug. 2013. Coupled Reversible and Irreversible Bistable Switches Underlying TGFβ-induced Epithelial to Mesenchymal Transition. Biophysical Journal 105 (4), 1079–1089.
URL http://linkinghub.elsevier.com/retrieve/pii/S0006349513007947

van Dassow, G., Eli Meir, Edwin M. Munro, Garrett M. Odell, Jul. 2000. The segment polarity network is a robust developmental model. Nature 406.

Veliz-Cuba, A., Stigler, B., Jun. 2011. Boolean Models Can Explain Bistability in the *lac* Operon. Journal of Computational Biology 18 (6), 783–794.
URL http://www.liebertonline.com/doi/abs/10.1089/cmb.2011.0031

Wang, R.-S., Saadatpour, A., Albert, R., 2012. Boolean modeling in systems biology: an overview of methodology and applications. Phys. Biol. 9 (5), 055001.
URL http://stacks.iop.org/1478-3975/9/i=5/a=055001

Wittmann, D. M., Krumsiek, J., Saez-Rodriguez, J., Lauffenburger, D. A., Klamt, S., Theis, F. J., 2009. Transforming Boolean models to continuous models: methodology and application to T-cell receptor signaling. BMC Systems Biology 3 (1), 98.
URL http://bmcsystbiol.biomedcentral.com/articles/10.1186/1752-0509-3-98

Yao, G., Tan, C., West, M., Nevins, J. R., You, L., Apr. 2014. Origin of bistability underlying mammalian cell cycle entry. Molecular Systems Biology 7 (1), 485–485.
URL http://msb.embopress.org/cgi/doi/10.1038/msb.2011.19

Yeger-Lotem, E., Sattath, S., Kashtan, N., Itzkovitz, S., Milo, R., Pinter, R. Y., Alon, U., Margalit, H., Apr. 2004. Network motifs in integrated cellular networks of transcription–regulation and protein–protein interaction. PNAS 101 (16), 5934–5939.
URL http://www.pnas.org/content/101/16/5934

Zañudo, J. G. T., Albert, R., Jun. 2013. An effective network reduction approach to find the dynamical repertoire of discrete dynamic networks. Chaos 23 (2), 025111.
URL http://aip.scitation.org/doi/10.1063/1.4809777

Zañudo, J. G. T., Albert, R., Apr. 2015. Cell Fate Reprogramming by Control of Intracellular Network Dynamics. PLOS Computational Biology 11 (4), e1004193.
URL http://journals.plos.org/ploscompbiol/article?id=10.1371/journal.pcbi.1004193